A&A 420, 729–736 (2004)
DOI: 10.1051/0004-6361:20041056

Astronomy & Astrophysics

The dynamical role of anomalous cosmic rays in the outer heliosphere

D. B. Alexashov[1], S. V. Chalov[1], A. V. Myasnikov[1], V. V. Izmodenov[2], and R. Kallenbach[3]

[1] Institute for Problems in Mechanics of the Russian Academy of Sciences, Prospect Vernadskogo 101-1, 119526 Moscow, Russia
[2] Moscow State University, Vorob'evy Gory, 119899 Moscow, Russia
[3] International Space Science Institute, Hallerstrasse 6, 3012 Bern, Switzerland

Received 19 January 2004 / Accepted 23 February 2004

Abstract. The two-dimensional model of the solar wind-local interstellar medium interaction developed by Baranov & Malama (1993, J. Geophys. Res., 98, 15 157) is improved by taking into account the dynamical effect of anomalous cosmic rays. The cosmic rays are treated as a massless diffusive fluid. It is shown that the termination shock shifts further away from the Sun in this case and the post-shock temperature of the thermal plasma decreases. The magnitude of the shift depends on the value of the energy-averaged spatial diffusion coefficient. The number density of energetic neutral hydrogen originating in the shocked solar wind is generally lower in the case of the cosmic-ray-modified termination shock.

Key words. acceleration of particles – Sun: solar wind – ISM: cosmic rays

1. Introduction

It has become evident within recent years that interstellar atoms have a pronounced effect on the physical properties of the solar wind flow in the outer heliosphere (e.g., Izmodenov 2000, 2001; Baranov 2003 and references therein). Apart from the fact that the position and shape of the termination shock and heliopause are significantly determined by the action of the atoms, they give rise to a distinctive hot population of pick-up ions in the solar wind. The pick-up ions are responsible for the origin of anomalous cosmic rays (ACRs) through the shock-drift and diffusive acceleration of the ions at the termination shock (Pesses et al. 1981; Jokipii 1992; Fichtner 2001). While the number density of ACRs is negligible compared to the thermal plasma number density throughout the heliosphere, their energy density downstream of the termination shock, in the present view, can be comparable to the energy density of the solar wind (Jokipii 1990; le Roux et al. 1996). Taking into account the effect of cosmic rays leads to a deceleration of the solar wind flow in front of the termination shock due to their pressure gradient and to a decrease in the compression ratio at the dissipative part of the shock (subshock). As a result the thermodynamical properties of the downstream plasma flow will differ from those in the case of the shock without cosmic rays. The structure of planar cosmic-ray-modified shocks has been the objective of extended studies. The extensive literature on these studies is reviewed by Zank (1999).

Send offprint requests to: S. V. Chalov, e-mail: chalov@ipmnet.ru

The effect of ACRs on the solar wind flow in geometry different from planar has been studied by Fahr et al. (1992), Ziemkiewicz (1994), Lee (1997), Banaszkiewicz & Ziemkiewicz (1997), Fahr et al. (2000) in the frame of the hydrodynamical approach for the cosmic-ray transport. Le Roux & Fichtner (1997a,b) and Berezhko & Ksenofontov (2003) have developed spherically symmetrical models of the termination shock in the framework of which the cosmic-ray transport is described by the kinetic diffusive equation.

In the present paper a two-dimensional model of the interaction between the solar wind and partially ionized interstellar medium taking into account the dynamical action of ACRs on the plasma flow is presented. In the framework of the model, thermal plasma and cosmic rays are treated as separate fluids, one of which (cosmic rays) is essentially diffusive, while neutral atoms (hydrogen) are described by the kinetic transport equation for their velocity distribution function. Interaction between the atoms and plasma is by the charge exchange reaction and electron impact ionization process. Our model is the extension of the well-known model by Baranov & Malama (1993) to the case when the effect of ACRs is included. The interplanetary magnetic field is not included in the model, that is, the diffusion coefficient of ACRs is assumed to be isotropic. However, the magnetic field close to the heliopause can have a pronounced effect on the transport of energetic particles in this region (Florinski et al. 2003).

2. Mathematical formulation of the problem

The coupled system of equations for thermal plasma and ACRs considered as a separate fluid with a negligible mass density has the form:

$$\frac{\partial \rho}{\partial t} + \nabla \cdot (\rho \boldsymbol{V}) = m_{\rm p} Q_1, \tag{1}$$

$$\frac{\partial}{\partial t}(\rho \boldsymbol{V}) + \nabla \cdot (\rho \boldsymbol{V} \otimes \boldsymbol{V}) + \nabla \left(p_{\rm g} + p_{\rm c}\right) = m_{\rm p} \boldsymbol{Q}_2, \tag{2}$$

$$\frac{\partial E_{\rm g}}{\partial t} + \nabla \cdot \left[\boldsymbol{V}\left(E_{\rm g} + p_{\rm g}\right)\right] = -\boldsymbol{V} \cdot \nabla p_{\rm c} + m_{\rm p} Q_3 + \alpha p_{\rm g} \nabla \cdot \boldsymbol{V}, \tag{3}$$

$$\frac{\partial E_{\rm c}}{\partial t} + \nabla \cdot \left[\boldsymbol{V}\left(E_{\rm c} + p_{\rm c}\right) - K \nabla E_{\rm c}\right] = \boldsymbol{V} \cdot \nabla p_{\rm c} - \alpha p_{\rm g} \nabla \cdot \boldsymbol{V}, \tag{4}$$

where ρ, $\boldsymbol{V}$, $p_{\rm g}$, and $E_{\rm g} = \rho V^2/2 + p_{\rm g}/(\gamma_{\rm g} - 1)$ are respectively the density, bulk velocity, pressure, and energy density of solar wind or interstellar thermal plasma, $E_{\rm c} = p_{\rm c}/(\gamma_{\rm c} - 1)$ is the energy density of cosmic rays, $p_{\rm c}$ is the cosmic-ray pressure, K is the isotropic energy-averaged diffusion coefficient which is assumed to be constant throughout, $\gamma_{\rm g}$ and $\gamma_{\rm c}$ are the respective adiabatic indexes of thermal plasma and cosmic rays, $m_{\rm p}$ is the proton mass. The last terms in Eqs. (3) and (4) determine energy loss and gain in thermal plasma and cosmic rays, respectively, due to the transfer of thermal protons to the ACR population. The transfer (injection) rate is assumed to depend on local values of the divergence of the solar wind flow and the thermal plasma pressure (e.g., Zank et al. 1993; Chalov & Fahr 1996, 1997; Fahr et al. 2000). The dimensionless parameter α determines the intensity of the injection. The terms Q_1, $\boldsymbol{Q}_2$, and Q_3 on the right hand side of Eqs. (1)–(3) are the mass, momentum, and energy sources in the thermal plasma component due to its interaction with hydrogen atoms. The terms can be written (e.g., Baranov & Malama 1993):

$$Q_1 = \beta n_{\rm H}, \quad n_{\rm H} = \int f_{\rm H}(\boldsymbol{w}_{\rm H})\, {\rm d}\boldsymbol{w}_{\rm H}, \tag{5}$$

$$\begin{aligned} \boldsymbol{Q}_2 \;=\; & \int \beta \boldsymbol{w}_{\rm H} f_{\rm H}(\boldsymbol{w}_{\rm H})\, {\rm d}\boldsymbol{w}_{\rm H} \\ & + \iint u \sigma_{\rm ex}^{\rm Hp}(u) \left(\boldsymbol{w}_{\rm H} - \boldsymbol{w}_{\rm p}\right) f_{\rm H}(\boldsymbol{w}_{\rm H})\, f_{\rm p}\left(\boldsymbol{w}_{\rm p}\right) {\rm d}\boldsymbol{w}_{\rm H} {\rm d}\boldsymbol{w}_{\rm p}, \end{aligned} \tag{6}$$

$$\begin{aligned} Q_3 \;=\; & \int \beta \frac{\boldsymbol{w}_{\rm H}^2}{2} f_{\rm H}(\boldsymbol{w}_{\rm H})\, {\rm d}\boldsymbol{w}_{\rm H} \\ & + \iint u \sigma_{\rm ex}^{\rm Hp}(u) \frac{\boldsymbol{w}_{\rm H}^2 - \boldsymbol{w}_{\rm p}^2}{2} f_{\rm H}(\boldsymbol{w}_{\rm H})\, f_{\rm p}\left(\boldsymbol{w}_{\rm p}\right) {\rm d}\boldsymbol{w}_{\rm H} {\rm d}\boldsymbol{w}_{\rm p}. \end{aligned} \tag{7}$$

In Eqs. (5)–(7) $f_{\rm p}(\boldsymbol{r}, \boldsymbol{w}_{\rm p})$ and $f_{\rm H}(\boldsymbol{r}, \boldsymbol{w}_{\rm H})$ are the velocity distribution functions of protons and hydrogen atoms, respectively, $n_{\rm H}$ is the number density of the atoms, $\sigma_{\rm ex}^{\rm Hp}$ is the charge exchange cross section of H atoms with protons, β is the sum of the photoionization and electron impact ionization rates, $u = |\boldsymbol{w}_{\rm H} - \boldsymbol{w}_{\rm p}|$ is the relative atom-proton velocity. The proton distribution function is assumed to be local Maxwellian, while the distribution function of atoms is a solution of the kinetic equation:

$$\begin{aligned} \boldsymbol{w}_{\rm H} \frac{\partial f_{\rm H}(\boldsymbol{r}, \boldsymbol{w}_{\rm H})}{\partial \boldsymbol{r}} \;+\; & \frac{\boldsymbol{F}}{m_{\rm H}} \frac{\partial f_{\rm H}(\boldsymbol{r}, \boldsymbol{w}_{\rm H})}{\partial \boldsymbol{w}_{\rm H}} = \\ & - f_{\rm H}(\boldsymbol{r}, \boldsymbol{w}_{\rm H}) \int |\boldsymbol{w}_{\rm H} - \boldsymbol{w}_{\rm p}| \sigma_{\rm ex}^{\rm Hp} f_{\rm p}\left(\boldsymbol{r}, \boldsymbol{w}_{\rm p}\right) {\rm d}\boldsymbol{w}_{\rm p} \\ & + f_{\rm p}(\boldsymbol{r}, \boldsymbol{w}_{\rm H}) \int |\boldsymbol{w}'_{\rm H} - \boldsymbol{w}_{\rm H}| \sigma_{\rm ex}^{\rm Hp} f_{\rm H}(\boldsymbol{r}, \boldsymbol{w}'_{\rm H})\, {\rm d}\boldsymbol{w}'_{\rm H} \\ & - \beta f_{\rm H}(\boldsymbol{r}, \boldsymbol{w}_{\rm H}), \end{aligned} \tag{8}$$

where $m_{\rm H}$ is the hydrogen atom mass and $\boldsymbol{F}$ is the sum of the solar gravitational and radiational pressure force.

Notice that a major step toward the development of a global self-consistent model of the solar wind interaction with the local interstellar medium (LISM) has been made by Fahr et al. (2000) who proposed a 5-fluid hydrodynamical approach taking into account solar and interstellar plasmas, pick-up ions, galactic cosmic rays, ACRs and interstellar atoms as separate fluid components. However, Fahr et al. (2000) use an expression for the pick-up ion pressure derived from the assumption that their velocity distribution function has a simple rectangular shape. Although this assumption can be justified in the supersonic solar wind, the velocity distribution function of pick-up ions has a very complex shape in regions behind the termination shock as was recently shown by Chalov et al. (2003). For example, the charge exchange reaction of pick-up ions and interstellar atoms results in the formation of gaps in their velocity distribution at medium energies, while compression of the plasma flow approaching the heliopause leads to formation of high-velocity tails. Since an adequate model taking into account the aforementioned processes is now in development, we prefer at this stage to consider solar wind plasma and pick-up ions as a single fluid.

It is generally accepted that injection of thermal protons into the ACR population takes place in the vicinity of the termination shock, that is, in the region of large gradients of the solar wind velocity. When accelerated at the termination shock, ACRs diffuse upstream and decelerate the solar wind flow in front of the shock, with the result that the precursor region followed by the subshock is formed. Since the precursor is believed to be rather steep, we assume here that the injection takes place both at the subshock and in the precursor. More precisely, in our calculations the last terms in Eqs. (3), (4) are taken into account beginning at distances upstream of the termination shock where the solar wind pressure starts to increase due to deceleration of the solar wind by the cosmic-ray pressure gradient. To gain better insight into the physical meaning of the injection rate, α, it is useful to relate it to the ratio of the energy injected in a unit of time near the shock front, q, and the downstream internal energy flux of thermal plasma, $\Phi_{\rm g}^{\rm d}$. With this aim in view, we consider a planar approximation for a cosmic-ray-modified shock assuming that the precursor is small in size compared to the curvature of the shock. One can obtain then from the one-dimensional version of Eq. (4) (for more detail see Chalov & Fahr 1997):

$$q \simeq \alpha \left(V_{\rm u} - V_{\rm d}\right) p_{\rm g}^{\rm d}/2, \tag{9}$$

where $V_{\rm u}$ and $V_{\rm d}$ are the upstream and downstream plasma velocities and $p_{\rm g}^{\rm d}$ is the downstream plasma pressure. It has been

taken into account to derive Eq. (9) that the downstream plasma pressure is much larger than the upstream one. The downstream internal energy flux of thermal plasma is

$$\Phi_{\rm g}^{\rm d} = \frac{\gamma_{\rm g}}{\gamma_{\rm g}-1} p_{\rm g}^{\rm d} V_{\rm d}. \tag{10}$$

It follows then from Eqs. (9) and (10) that

$$\eta = \frac{\alpha\left(\gamma_{\rm g}-1\right)}{2\gamma_{\rm g}}\left(\sigma-1\right), \tag{11}$$

where $\eta = q/\Phi_{\rm g}^{\rm d}$ and $\sigma = V_{\rm u}/V_{\rm d}$ is the total compression ratio at the shock. As indicated above, the term $p_{\rm g}$ in Eqs. (9) and (10) is the total pressure of the mixture of solar wind plasma and pick-up ions. Although only pick-up ions are considered to be the source of ACRs, nevertheless the value η describes the injection process reasonably well, since it shows the fraction of the downstream thermal energy transferred to ACRs without specifying an injection mechanism. At present, there is no consensus of opinion regarding the injection mechanism at the termination shock, and it is beyond the scope of this paper. The pick-up ion pressure downstream of the termination shock is comparable with the solar wind pressure and, possibly, even exceeds it. Thus the pick-up ions contribute significantly to the total pressure $p_{\rm g}^{\rm d}$.

To solve the system of Eqs. (1)–(8) which govern the interaction of the solar wind with the partly ionized interstellar medium in the framework of the hybrid model treating hydrogen atoms kinetically and charged components as fluids, the method of global iterations has been applied (Baranov et al. 1991; Baranov & Malama 1993). At the first iteration, distributions of the thermal plasma and ACR parameters resulting from solution of Eqs. (1)–(4) with $\boldsymbol{Q} = 0$ are found. To solve Eqs. (1)–(4) the soft fitting technique has been used. When coupled with the method of physical process splitting, the soft fitting technique allows us to take into account different physical processes and study their influence on the plasma flow. The corresponding numerical algorithm is outlined by Myasnikov et al. (2000a,b). Since the soft fitting technique allows us to approximately fit discontinuities, the Monte Carlo method with splitting of trajectories (Malama 1991) has been then directly applied to solve the kinetic equation for the motion of hydrogen atoms (Eq. (8)). Then the term $\boldsymbol{Q}$ is calculated and used thereafter to find plasma and ACR distributions in the next iteration. The new plasma distributions are, in turn, the basis for the next Monte Carlo simulation of hydrogen atom trajectories and for calculation of new source terms. The iterative process continues until the thermal plasma, cosmic rays and neutral atom distributions are independent of the iteration number.

In the undisturbed interstellar medium the velocity distribution function $f_{\rm H}$ is assumed to be Maxwellian. Since the radial gradients of ACRs are small in the inner heliosphere and since we are interested here in the global distribution of ACRs in the region of the solar wind and LISM interaction, it is a good approximation to assume that at 1 AU the condition $\nabla p_{\rm c} = 0$ is satisfied.

3. Properties of cosmic-ray-modified shock waves of finite size

Before proceeding to a presentation of results of numerical calculations, we consider general properties of finite-size shock waves producing cosmic rays. We consider a one-dimensional structure of a planar cosmic-ray-modified shock. In general, a diffusive shock wave in a mixture of thermal plasma and cosmic rays consists of a dissipative plasma subshock and a smooth precursor formed when cosmic rays scatter upstream of the subshock. For the sake of simplicity we ignore in this section effects of neutral atoms and assume that injection of cosmic rays takes place at the subshock only. Then the plasma flow in the precursor region is governed by the one-dimensional version of Eqs. (1)–(4) with $\boldsymbol{Q} = 0$ and $\alpha = 0$, while the following jump relations are fulfilled at the subshock (see Chalov & Fahr 1997):

$$[\rho V] = 0, \tag{12}$$

$$\left[\rho V^2 + p_{\rm g}\right] = 0, \tag{13}$$

$$\left[V\left(E_{\rm g} + p_{\rm g}\right) + F_{\rm c}\right] = 0, \tag{14}$$

$$[p_{\rm c}] = 0, \qquad [F_{\rm c}] = q, \tag{15}$$

where

$$F_{\rm c} = \frac{\gamma_{\rm c}}{\gamma_{\rm c}-1} p_{\rm c} V - \frac{K}{\gamma_{\rm c}-1}\frac{{\rm d}p_{\rm c}}{{\rm d}x}, \tag{16}$$

$$q = \lim_{\varepsilon\to 0}\int_{-\epsilon}^{\epsilon}\left(-\alpha p_{\rm g}\frac{{\rm d}V}{{\rm d}x}\right){\rm d}x = -\frac{\alpha}{2}\left(p_{\rm g}^{\rm u} + p_{\rm g}^{\rm d}\right)\left(V_{\rm d} - V_{\rm u}\right). \tag{17}$$

Here the subshock position is defined as $x = 0$; $V_{\rm u}(V_{\rm d})$ and $p_{\rm g}^{\rm u}(p_{\rm g}^{\rm d})$ are the plasma speed (positive) and pressure in front of (behind) the subshock, respectively. The difference between Eqs. (17) and (9) is that injection both in the precursor and at the subshock is taken into account in Eq. (9).

To model the finite size of the shock front we assume that a free escape boundary is located at distance L upstream of the subshock, that is

$$p_{\rm c}\left(x \le -L\right) = 0. \tag{18}$$

Thus, in the case of finite-size shocks some fraction of energetic particles can escape upstream and carry away some portion of the energy. As a result of the energy losses the total compression ratio at cosmic-ray-modified shocks can increase. Figure 1 shows the compression ratio at the subshock and the total compression ratio at a planar cosmic-ray-modified shock with the free escape boundary as functions of dimensionless diffusion coefficient $\hat{K} = K/LV_{\rm L}$ at $M_{\rm g}^{\rm L} = \sqrt{\rho_{\rm L}V_{\rm L}^2/\gamma_{\rm g}p_{\rm g}^{\rm L}} = 3$ and $\alpha = 0.1$, where the subscript and superscript "L" shows that the values of corresponding functions are taken at $x = -L$. It is evident that the dimensionless diffusion coefficient equals the ratio of the diffusive length scale $L_{\rm D} = K/V_{\rm L}$ and characteristic size of the shock L. At small values of $\hat{K}$ the properties of the shock are the same as in the case of a shock which is infinite in size. Acceleration of cosmic rays is very efficient in

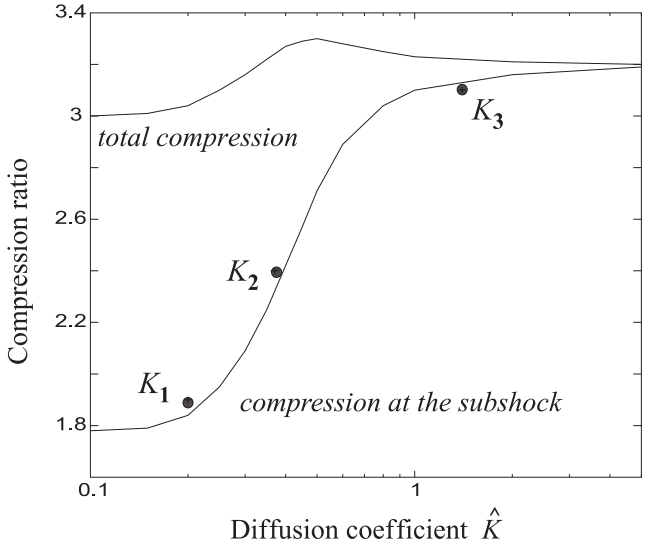

Fig. 1. The compression ratio at the subshock and total compression ratio as functions of the dimensionless diffusion coefficient $\hat{K}$. The filled circles show calculated compression ratios at the subshock in the upwind direction in the frame of the two-dimensional model (see Sect. 4).

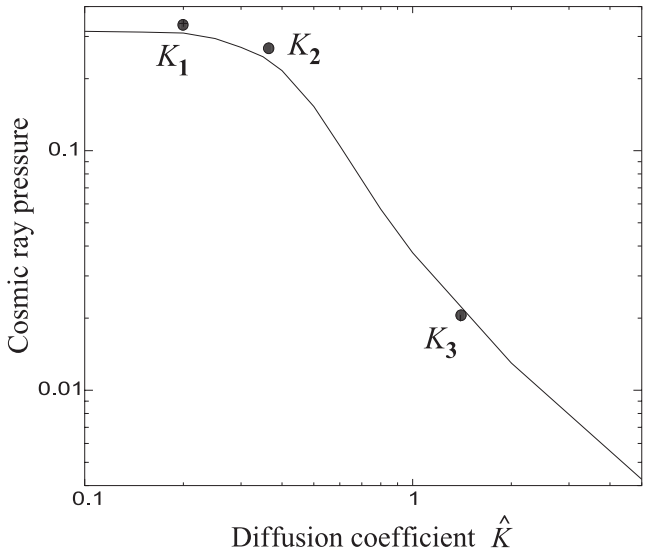

Fig. 2. The cosmic-ray pressure at the subshock in units of $\rho_L V_L^2$ as a function of the dimensionless diffusion coeficient $\hat{K}$. The filled circles show calculated pressures in the upwind direction in the frame of the two-dimensional model (see Sect. 4).

this case and their pressure is high, as shown in Fig. 2. As a result the shock wave is strongly modified by the cosmic-ray pressure and the compression ratio at the subshock is relatively small compared to the total compression ratio. The compression ratio at the subshock increases and the cosmic-ray pressure decreases with increasing $\hat{K}$ due to escape of energetic particles from the vicinity of the shock front. At $L_D \gtrsim L$ the precursor is practically absent. On the other hand, the energy losses result in an increase of the total compression ratio at large values of $\hat{K}$.

The properties of cosmic-ray-modified shock waves will be used in the subsequent discussion of numerical results concerning the solar wind termination shock.

4. Spatial distributions of thermal plasma, hydrogen atoms and ACRs in the cosmic-ray-modified heliosphere

According to present knowledge on parameters of the LISM, the following values for the plasma bulk speed, proton number density, neutral hydrogen number density and plasma Mach number of unperturbed interstellar medium have been chosen in our calculations: $V_{LISM} = 25$ km s^{-1}, $n_{p,LISM} = 0.07$ cm^{-3}, $n_{H,LISM} = 0.2$ cm^{-3}, $M_{LISM} = 2$. Concerning the solar wind parameters the following values have been adopted at 1 AU: $V_E = 450$ km s^{-1}, $n_{p,E} = 7$ cm^{-3}, $M_E = 10$. Under these conditions in the case when dynamical influence of ACRs on the plasma flow is not taken into account, the upwind position of the termination shock and heliopause is 99.6 AU and 176 AU, respectively. The compression ratio at the termination shock equals 2.97. Such a low value of the compression ratio is connected to heating of the distant solar wind due to production of pick-up protons which in the framework of our model have assimilated completely in the solar wind.

Throughout the present paper the injection rate of ACRs is fixed, $\alpha = 0.1$, while the value of the diffusion coefficient is considered as a free parameter. It follows from Eq. (4) that the adopted value of α corresponds to $\eta \approx 0.04$. This means that the energy injected in ACRs near the termination shock is equal to 4% of the downstream internal energy of thermal plasma. This value of the injection rate falls in the range between the low injection efficiency and high efficiency considered by le Roux & Fichtner (1997a,b). The adiabatic indexes of thermal plasma and cosmic rays are assumed to equal $\gamma_g = \gamma_c = 5/3$.

Figure 3 shows upwind positions of the termination shock and solar wind speed near the shock for three different values of the diffusion coefficient: 1) $K_1 = 3.75 \times 10^{20}$ cm s^{-1} (curve 1); 2) $K_2 = 3.75 \times 10^{21}$ cm s^{-1} (curve 2); 3) $K_3 = 3.75 \times 10^{22}$ cm s^{-1} (curve 3). Curve 4 shows the position of the termination shock without ACRs. We consider here the range of the diffusion coefficients due to uncertainties of their values in the outer heliosphere and possible variations with the solar cycle. The effect of ACRs on the solar wind plasma flow leads to formation of a smooth region of solar wind deceleration (precursor), followed by the subshock, and to a shift of the subshock towards larger distance. The intensity of the subshock and the value of the shift depend on the value of the diffusion coefficient with the largest shift occurring at medium values of K. To account for the features of the termination shock shown in Fig. 3, we refer to the results obtained in Sect. 3. The main difficulty encountered in comparing a one-dimensional shock with the free escape boundary and the termination shock is correct determination of the distance to the free escape boundary, L. The assumption that L equals simply the distance from the Sun to the termination shock can be too rough, since energy losses in the case of the termination shock can be connected not only to escape of energetic particles from the vicinity of the shock front due to its finite size, but to adiabatic cooling

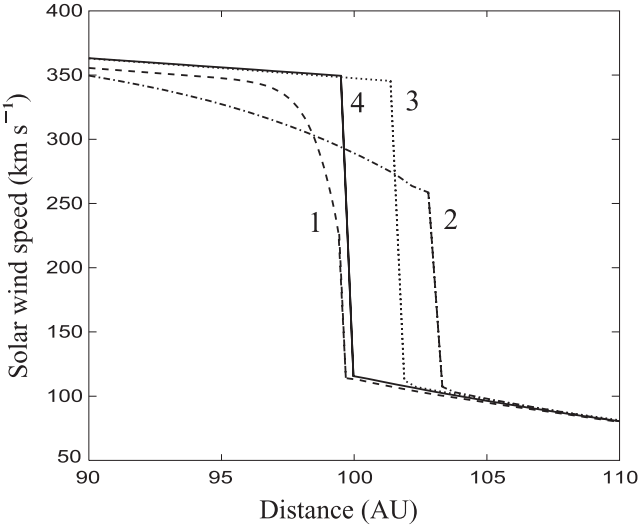

Fig. 3. Upwind positions of the termination shock for three different values of the diffusion coefficient: 1) $K_1 = 3.75{\times}10^{20}$ cm s^{-1} (curve 1); 2) $K_2 = 3.75 \times 10^{21}$ cm s^{-1} (curve 2); 3) $K_3 = 3.75 \times 10^{22}$ cm s^{-1} (curve 3). Curve 4 shows the position of the shock in the case when ACRs absent. The precursor is pronounced at small and medium values of K.

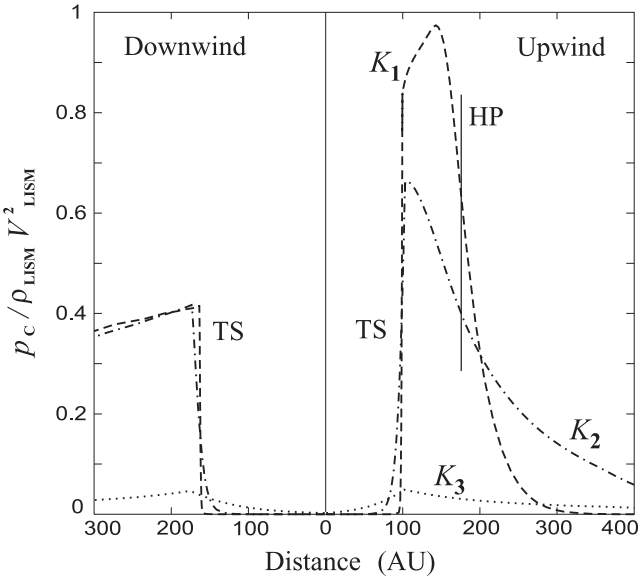

Fig. 4. The cosmic-ray pressure in units of $\rho_{\rm LISM} V^2_{\rm LISM}$ in the upwind and downwind directions at $K = K_1$ (dashed lines), $K = K_2$ (dotted-dashed lines), and $K = K_3$ (dotted lines). The positions of the termination shock (TS) and heliopause (HP) are shown.

Table 1. Diffusion coefficients and distances to the free escape boundary.

K(cm^2 s^{-1})	L(AU)	$\hat{K}$
3.75×10^{20}	4	0.2
3.75×10^{21}	21	0.37
3.75×10^{22}	56	1.4

in expanding solar wind as well. Thus, we can expect that L is less than the heliocentric distance to the shock. To estimate the value of L the following procedure is used. First we calculate analytically the cosmic-ray pressure at a spherical shock wave in linear approximation (backreaction of the cosmic rays is not taken into account). The radius of the shock and compression ratio are the same as for the termination shock. Then we calculate the cosmic-ray pressure in a linear approximation at a planar shock with the free escape boundary and the same parameters as in the case of the spherical shock. In both cases the values of the diffusion coefficient and injection rate are identical. By the variation of the distance from the planar shock to the free escape boundary we find the value of L that results in equal cosmic-ray pressures at the planar and spherical shocks. Table 1 shows calculated L and corresponding values of the dimensionless diffusion coefficient $\hat{K}$ for different K. The solar wind speed in front of the termination shock in the case without ACRs which has been used to calculate $\hat{K}$ equals 320 km s^{-1}. Such a low value of the speed in the outer heliosphere is due to deceleration of the solar wind by interstellar hydrogen atoms.

Turning back to Fig. 3, we see that the compression ratios at the subshocks are in good qualitative accordance with the results of the simplified one-dimensional model presented in Sect. 3. In Fig. 1 these compression ratios are shown as the filled circles for the three values of the diffusion coefficient under consideration. Now the positions of the subshocks can be easily understood. The position of the termination shock is governed by the balance between the interstellar and post-shock pressures. The smaller the heliocentric distance of the shock and the larger the compression ratio, the larger the downstream pressure. Thus, an increase of the total compression ratio at the shock results in an increase of its heliocentric distance. The largest total compression is at medium values of the diffusion coefficient as seen in Fig. 1. That is why the maximum shift of the termination shock in Fig. 3 corresponds to $K = K_2$. Note that the heliocentric distance of the shock at $K = K_1$ and in the case without ACRs is the same within the accuracy of the numerical code. The increase of the heliocentric distance of the ACR-modified termination shock due to the increase of the total compression ratio has been also demonstrated by Berezhko & Ksenofontov (2003) in the framework of a one-dimensional spherically symmetric model of the termination shock with the kinetic description of the cosmic-ray transport. Le Roux & Fichtner (1997b) also obtained the shift of the termination shock position towards larger distances in the case when the effect of ACRs is taken into account. However, they obtained a smaller total compression ratio for the cosmic-ray-modified shock compared to the shock without ACRs (see Fig. 4 in the above-mentioned paper). This result is in contradiction to our present findings and the results presented by Berezhko & Ksenofontov (2003).

Figure 4 shows the spatial distributions of the ACR pressure in the upwind and downwind directions for different values of the diffusion coefficient. The pressure in the upwind direction decreases with increasing diffusion coefficient, as expected from the one-dimensional model (see Fig. 2). In the downwind direction the cosmic-ray pressures at $K = K_1$ and $K = K_2$ are approximately equal. This can be explained with Fig. 2. The heliocentric distance to the termination shock in the downwind

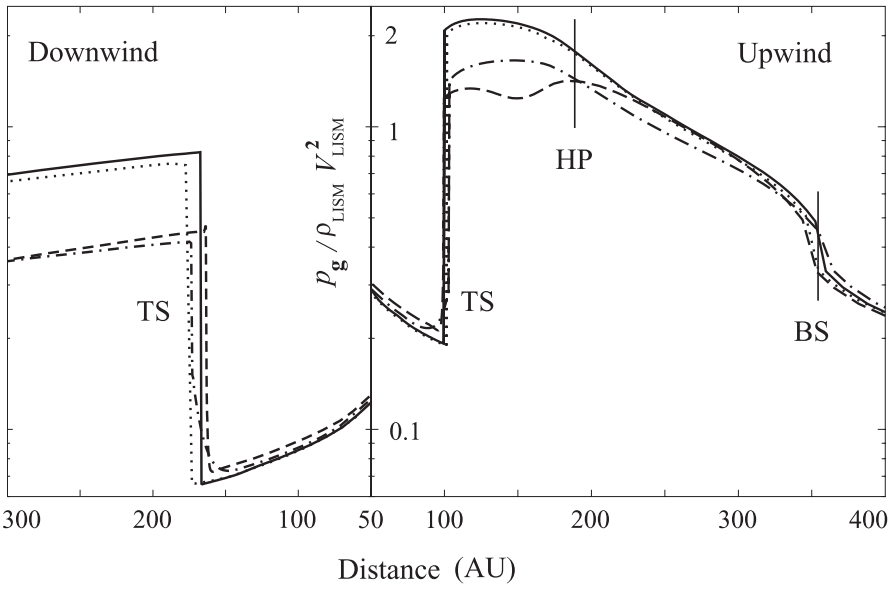

Fig. 5. The pressure of thermal plasma in units of $\rho_{\rm LISM} V_{\rm LISM}^2$ in the upwind and downwind directions at $K = K_1$ (dashed lines), $K = K_2$ (dotted-dashed lines), and $K = K_3$ (dotted lines). The solid lines show the pressure in the case when are ACRs absent. The positions of the termination shock (TS), heliopause (HP), and bow shock (BS) are shown.

direction is more than that in the upwind direction by a factor of 1.7. This results in an increase in L and hence in an decrease in $\hat{K}$. As is seen from Fig. 2, due to the decrease of $\hat{K}_1$ and $\hat{K}_2$ these values fall on the plateau region of the cosmic-ray pressure distribution with a very small pressure gradient. It should be pointed out also that the cosmic-ray pressure at the termination shock in the downwind direction is lower than in the upwind one, even though the intensities of the shock are approximately the same in both directions. This behaviour of the cosmic-ray pressure is directly connected to the fact that the solar wind pressure both upstream and downstream of the termination shock is larger in the upwind direction compared to the downstream one (see Fig. 5). Then, as is evident from Eq. (4), the energy gain in ACRs due to injection of thermal protons at the shock will be larger in the upwind direction.

The modification of the solar wind flow by ACRs has a minor effect on the spatial distribution of interstellar hydrogen atoms in the heliosphere. However, the effect on the spatial distribution of hydrogen atoms originating in the region between the termination shock and heliopause (inner heliosheath) due to charge exchange of interstellar hydrogen with solar wind protons is rather pronounced. Figure 6 shows the spatial distributions of these atoms in the upwind and downwind directions, respectively. The solid curve corresponds to the case without cosmic rays and the dashed, dotted-dashed, and dotted curves represent distributions with $K = K_1$, $K = K_2$, and $K = K_3$, respectively. It is seen from Fig. 6 that the effect of ACRs can result in a decrease of the number density of the secondary hydrogen atoms originating in the inner heliosheath to 50% depending on the value of the diffusion coefficient. The smaller the diffusion coefficient, the greater is the decrease. The decrease of the number density can be explained by a decrease of the postshock plasma temperature in the case of cosmic-ray-modified shocks due to changes in the dissipative subshock intensity as discussed above. Figure 7 illustrates the dependence of the postshock temperature on the value of the diffusion coefficient. The smaller the diffusion coefficient, the lower is the temperature. In turn at the low temperatures downstream of the

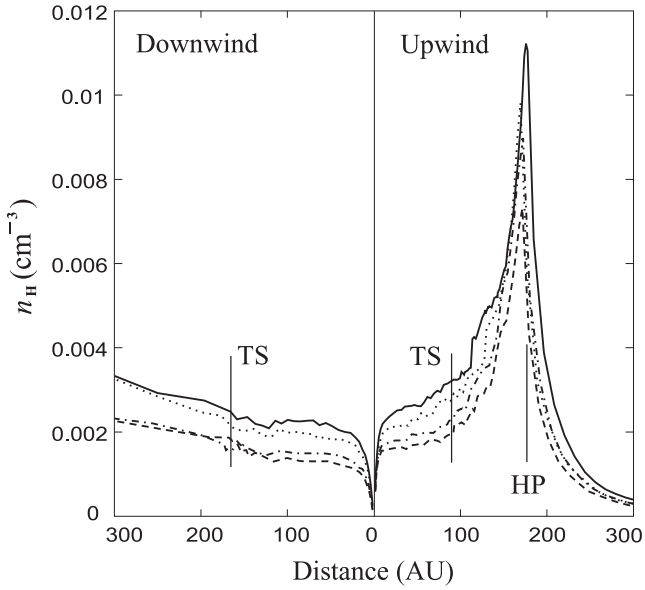

Fig. 6. The number density of hydrogen atoms originating in the shocked solar wind at $K = K_1$ (dashed lines), $K = K_2$ (dotted-dashed lines), and $K = K_3$ (dotted lines). The solid lines show the number density in the case when are ACRs absent.

termination shock the ionization rate of interstellar atoms by electron impact is lower compared to the shock without ACRs and hence the number density of solar wind protons is lower as well. Note here that the importance of the ionization by electron impact in shocked solar wind plasma has been emphasized by Baranov & Malama (1996). Since the production rate of the secondary atoms depends on the number density of solar wind protons in the inner heliosheath, the number density of the atoms will be lower in the case of the termination shock modified by ACRs in comparison to the shock without ACRs, in accordance with the results presented in Fig. 6.

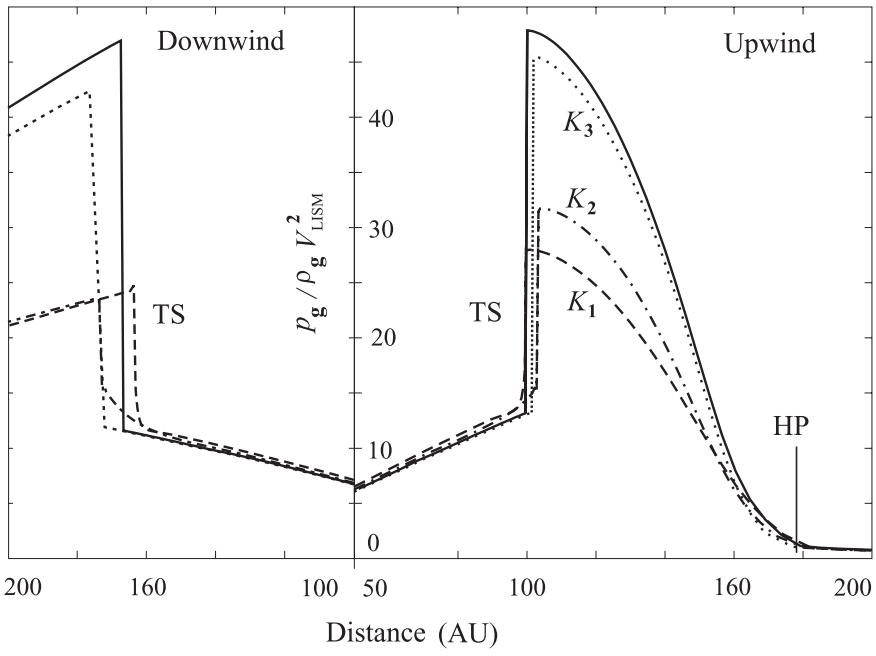

Fig. 7. The normalized temperature of the thermal plasma in the upwind and downwind directions at different values of the diffusion coefficient. Solid lines show the temperature in the case when are ACRs absent.

5. Conclusions

The dynamical influence of ACRs on the solar wind flow in the outer heliosphere and on the structure of the termination shock has been studied in the present paper in the framework of the self-consistent two-dimensional model of the interaction between the solar wind and partially ionized interstellar medium. Whereas earlier researches of the cosmic-ray-modified heliosphere were devoted mainly to the dependence of the termination shock structure and position on the injection rate of ACRs, we studied here effects connected to changes in the value of the diffusion coefficient keeping the injection rate fixed. Different values of the diffusion coefficient are considered because K is poorly known in the outer heliosphere and especially in the heliosheath, and in addition the value of the diffusion coefficient varies with the solar cycle. It has been shown in the paper that

1. The effect of ACRs on the solar wind flow near the termination shock leads to formation of a smooth precursor, followed by the subshock, and to a shift of the subshock towards larger distances in the upwind direction. This result is consistent with other findings (Ziemkiewicz 1994; Lee 1997; Banaszkiewicz & Ziemkiewicz 1997; le Roux & Fichtner 1997b; Berezhko & Ksenofontov 2003) based on one-dimensional spherically symmetric models. The intensity of the subshock and the magnitude of the shift depend on the value of the diffusion coefficient with the largest shift (about 4 AU) occurring at medium values of K.
2. The precursor of the termination shock is rather pronounced except for the case with large K. It has been shown by Berezhko (1986), Chalov (1988a,b) and Zank et al. (1990) that the precursor of a cosmic-ray-modified shock is highly unstable with respect to magnetosonic disturbances if the cosmic-ray pressure gradient in the precursor is sufficiently large. The possible detection of oscillations in the magnetic field and solar wind speed by the Voyager spacecraft in the near future could be evidence for the termination shock. The oscillations connected with the instability of the precursor have the distinctive feature: the magnetic field in more unstable modes oscillates in the longitudinal direction, while the solar wind speed oscillates in the direction perpendicular to the ecliptic plane (Chalov 1990).
3. The postshock temperature of the solar wind plasma is lower in the case of the cosmic-ray-modified termination shock compared to the shock without ACRs. The decrease in the temperature results in a decrease in the number density of hydrogen atoms originating in the region between the termination shock and heliopause. This result is of importance for the interpretation of energetic neutral atom (ENA) fluxes from the inner heliosheath observed with SOHO/CELIAS (Hilchenbach et al. 1998). It has been known that the ENAs can give important new information on the parameters of the solar wind plasma in the inner heliosheath and on the structure of the termination shock (e.g., Gruntman et al. 2001; Chalov et al. 2003).
4. The cosmic-ray pressure downstream of the termination shock is comparable with the thermal plasma pressure for small K when the diffusive length scale is much smaller than the distance to the shock. On the other hand, at large K the postshock cosmic-ray pressure is negligible compared to the thermal plasma pressure. There is pronounced upwind-downwind asymmetry in the cosmic-ray energy distribution due to difference in the amount of energy injected in ACRs in the up- and downwind parts of the termination shock. This difference in the injected energy is connected to the fact that the thermal plasma pressure is lower in the downwind part of the shock compared to the upwind part (see the last term in Eq. (4)). This kind of asymmetry has also been pointed out by Fahr et al. (1992, 2000).

Acknowledgements. This work was supported in part by INTAS cooperation project 2001-0270, Russian Foundation for Basic

Research (RFBR) grants 03-02-04020, 04-01-00594, 04-02-16559, and Program of Basic Researches of OEMMPU RAN.

References

Banaszkiewicz, M., & Ziemkiewicz, J. 1997, A&A, 327, 392
Baranov, V. B. 2003, in Solar Wind Ten, ed. M. Velli, R. Bruno, & F. Malara (AIP), 21
Baranov, V. B., & Malama, Y. G. 1993, J. Geophys. Res., 98, 15157
Baranov, V. B., & Malama, Y. G. 1996, Space Sci. Rev., 78, 305
Baranov, V. B., Lebedev, M. G., & Malama, Y. G. 1991, ApJ, 375, 347
Berezhko, E. G., & Ksenofontov, L. T. 2003, in Proc. 28th Int. Cosmic Ray Conf., in press
Berezhko, E. G. 1986, SvAL, 12, 352
Chalov, S. V. 1988a, SvAL, 14, 114
Chalov, S. V. 1988b, Ap&SS, 148, 175
Chalov, S. V. 1990, in Physics of the Outer Heliosphere, ed. S. Grzedzielski, & D. E. Page (Pergamon), 219
Chalov, S. V., & Fahr, H. J. 1996, A&A, 311, 317
Chalov, S. V., & Fahr, H. J. 1997, A&A, 326, 860
Chalov, S. V., Fahr, H. J., & Izmodenov, V. V. 2003, J. Geophys. Res., 108, 1266
Fahr, H. J., Fichtner, H., & Grzedzielski, S. 1992, Sol. Phys., 137, 355
Fahr, H. J., Kausch, T., & Scherer, H. 2000, A&A, 357, 268
Fichtner, H. 2001, Space Sci. Rev., 95, 639
Florinski, V., Zank, G. P., & Pogorelov, N. V. 2003, J. Geophys. Res., 108, 1228
Gruntman, M., Roelof, E. C., Mitchell, D. G., et al. 2001, J. Geophys. Res., 106, 15767
Hilchenbach, M., Hsieh, K. C., Hovestadt, D., et al. 1998, ApJ, 503, 916
Izmodenov, V. V. 2000, Ap&SS, 274, 55
Izmodenov, V. V. 2001, in The Outer Heliosphere: The Next Frontiers, ed. K. Scherer, H. Fichtner, H. Fahr, & E. Marsh (Pergamon), 23
Jokipii, J. R. 1990, in Physics of the Outer Heliosphere, ed. S. Grzedzielski, & D. E. Page (Pergamon), 169
Jokipii, J. R. 1992, ApJ, 393, L41
Lee, M. A. 1997, in Cosmic Winds and the Heliosphere, ed. J. R. Jokipii, C. P. Sonett, & M. S. Giampapa (Universal Arizona press), 857
le Roux, J. A., & Fichtner, H. 1997a, ApJ, 477, L115
le Roux, J. A., & Fichtner, H. 1997b, J. Geophys. Res., 102, 17365
le Roux, J. A., Potgieter, M. S., & Ptuskin, V. S. 1996, J. Geophys. Res., 101, 4791
Malama, Y. G. 1991, Ap&SS, 176, 21
Myasnikov, A. V., Izmodenov, V. V., Alexashov, D. B., & Chalov, S. V. 2000a, J. Geophys. Res., 105, 5167
Myasnikov, A. V., Izmodenov, V. V., Alexashov, D. B., & Chalov, S. V. 2000b, J. Geophys. Res., 105, 5179
Pesses, M. E., Jokipii, J. R., & Eichler, D. 1981, ApJ, 246, L85
Zank, G. 1999, Space Sci. Rev., 89, 413
Zank, G. P., Axford, W. I., & McKenzie, J. F. 1990, A&A, 233, 275
Zank, G. P., Webb, G. M., & Donohue, D. J. 1993, ApJ, 406, 67
Ziemkiewicz, J. 1994, A&A, 292, 677